

Monitoring Committee Progress Report #3

Numerical Representation of Mountains in Atmospheric Models

James Shaw

Supervisors: Hilary Weller, John Methven, Terry Davies

Monitoring Committee: Maarten Ambaum, Paul Williams

31st May 2016

1 Introduction

Next-generation atmospheric models are designed to be more flexible than previous models, so that the choice of mesh and choices of numerical schemes can be deferred or changed during operation (Ford et al., 2013; Theurich et al., 2015). My PhD project seeks to make numerical weather and climate predictions more accurate by developing new meshes and numerical schemes that are suitable for next-generation models. In particular, the project addresses the modelling of orographic flows on arbitrary meshes, focusing on three aspects: first, how orography is best represented by a mesh; second, how to accurately advect quantities over orography and, third, how to avoid unphysical solutions in the vertical balance between pressure and temperature.

Representing orography with meshes

There are two main types of mesh used in atmospheric models: terrain-following meshes and cut cells meshes. Terrain-following meshes reduce numerical accuracy in the calculation of horizontal pressure gradients (Gary, 1973; Zängl, 2012) and advection terms (Schär et al., 2002). Inaccuracies are larger near steep terrain. Cut cell meshes are an alternative to terrain-following meshes. Cut cell meshes are orthogonal everywhere except at the surface so that pressure gradient errors and advection errors are reduced, especially near steep terrain (Lock et al., 2012; Good et al., 2014). However, cut cell meshes can have arbitrarily small cells which impose severe constraints on the timestep for explicit methods (Almgren et al., 1997).

To illustrate the two types of mesh, a wave-shaped mountain with a peak height of 1 km is represented using a basic terrain-following mesh (figure 1a) and a cut cell mesh (figure 1b). Notice that the basic terrain-following mesh is severely distorted over steep surfaces while, on the cut cell mesh, small cells are found near the mountain peak. The development of a new type of mesh, the slanted cell mesh, is discussed in section 2.

Advection on arbitrary meshes

When a wind field is misaligned with the mesh, an advection scheme must account for transverse flux between diagonally adjacent cells (Clappier, 1998). Dimensionally split schemes that do not account for transverse fluxes can distort advected quantities (Leonard et al., 1993). These distortions are called ‘splitting errors’. In contrast, multidimensional schemes naturally account for such fluxes by including cross terms in the flux calculations (Leonard et al., 1993).

Dimensionally split schemes are attractive because they are often computationally efficient compared to multidimensional schemes (Bott, 2010), and a number of improvements have been developed to

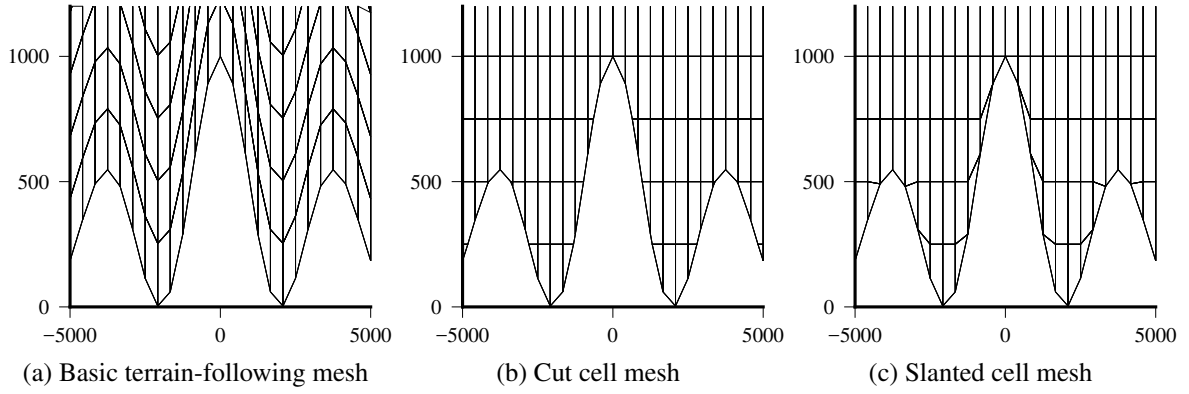


Figure 1: Cell edges of basic terrain-following, cut cell and slanted cell meshes having the same wave-shaped mountain profile. Only the lowest 1.2 km in the centre of the domain is shown. The entire domain is 300 km wide and 30 km high. Axis units are m. Cut cell mesh generated with code kindly provided by TROPOS.

alleviate splitting errors (Leonard et al., 1996; Bott, 2010). The advection scheme by Weller and Shahrokhi (2014) is a multidimensional scheme that achieves computational efficiency by precomputing fluxes using the mesh geometry only. Some aspects of this scheme are being modified to improve stability and accuracy, and this is the subject of section 3.

Vertical balance on arbitrary meshes

Some numerical models are susceptible to computational modes which produce unphysical solutions. Models that have a Lorenz vertical staggering of variables can suffer from one such computational mode (Arakawa and Konor, 1996). The Charney–Phillips vertical staggering does not suffer from the Lorenz computational mode, but it has only been formulated on structured, quadrilateral meshes. I intend to develop a generalisation of the Charney–Phillips staggering for arbitrary meshes, and the necessary tasks are outlined in section 4.

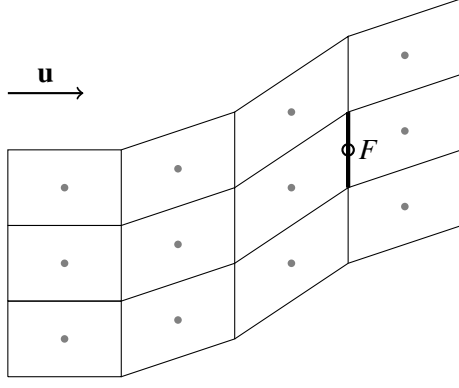
2 Comparison of terrain-following and slanted cell meshes

During the first year of my PhD, I compared the numerical accuracy on terrain-following and slanted cell meshes. In the second monitoring committee report (called MC2 hereafter), a slanted cell mesh was referred to as a cut cell mesh, but it is necessary to make a distinction between the two types: the differences can be seen by comparing the representation of the same terrain profile using cut cells (figure 1b) and slanted cells (figure 1c).

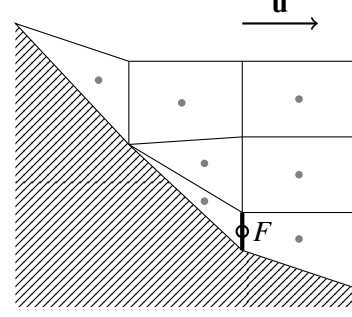
The slanted cell method has advantages over the cut cell method. First, unlike the construction of cut cell meshes, which can be somewhat involved (Hartkopf, 2011), I have developed a new technique that makes slanted cell meshes straightforward to construct (Shaw and Weller, 2016). Second, the slanted cell method does not severely constrain the timestep because thin cells are created that are long in the direction of flow.

The Leibniz Institute for Tropospheric Research (TROPOS) have kindly provided me with their cut cell mesh generator used in the All Scale Atmospheric Model (Jähn et al., 2015). This generates true cut cell meshes and will enable me to compare results on cut cell and slanted cell meshes.

Our submission to Monthly Weather Review underwent a third round of major revisions that included the development of a new slanted cell method which avoided the complex heuristics employed by the previous method (see MC2, section 3). The article was accepted for publication in February 2016 and is now undergoing prepress proofing.



(a) 12-point stencil in the domain interior



(b) 7-point stencil near the lower boundary of a slanted cell mesh. The ground is shown with diagonal hatching.

Figure 2: Two-dimensional stencils used for approximating a value at a face centroid given a set of surrounding cell centre values. In the two stencils, the face F is shown with a thick line, and the face centroid with an open circle. Cell centres are denoted by grey filled circles. The direction of the windvector, \mathbf{u} , is shown above both stencils.

3 Improving advection on slanted cell meshes

My current work focuses on improving the stability of a multidimensional advection scheme that is suitable for arbitrary meshes (Weller and Shahrokhi, 2014). The performance of the advection scheme is being evaluated over steep slopes on terrain-following, cut cell and slanted cell meshes.

The multidimensional advection scheme is an explicit, Eulerian, finite-volume scheme that has a cubic upwind-biased stencil. Fluxes across faces are approximated using a least squares polynomial fit onto the stencil point values. On a two-dimensional quadrilateral mesh, the stencil has 4×3 points in the domain interior (figure 2a), but may include fewer points near the boundaries. This is a particular concern at the lower boundary where stencils may be smaller and highly distorted (figure 2b).

In the interior of a two-dimensional domain, we fit a polynomial surface to a stencil of a discrete scalar field ϕ :

$$\phi = a_1 + a_2x + a_3y + a_4x^2 + a_5xy + a_6y^2 + a_7x^3 + a_8x^2y + a_9xy^2 \quad (1)$$

where $a_1 \dots a_9$ are the unknown coefficients that are calculated from the least squares fit. It may not be possible to fit all the polynomial terms to a stencil near the lower boundary because it includes fewer points. With help from Philip Browne, I have developed a mathematical technique that removes certain high-order terms based on the stencil geometry. We call this technique an ‘adaptive polynomial fit’.

The adaptive polynomial fit alone is not enough to ensure numerical stability. I am developing a new procedure that will stabilise the polynomial fit for troublesome stencils. It is based on constraints derived from a one-dimensional von Neumann analysis of a simplified version of the spatial discretisation. Compared to the original version of the advection scheme by Weller and Shahrokhi (2014), the improved version is stable for a wider range of test cases and has accuracy that is comparable to the original version. However, the scheme is weakly unstable in certain cases (figure 3) and a solution has yet to be found. Further work is needed to give us confidence that the scheme is stable and accurate for arbitrary meshes. I am working with Tristan Pryer here at Reading, and I am reaching out to other experts in the field for suggestions.

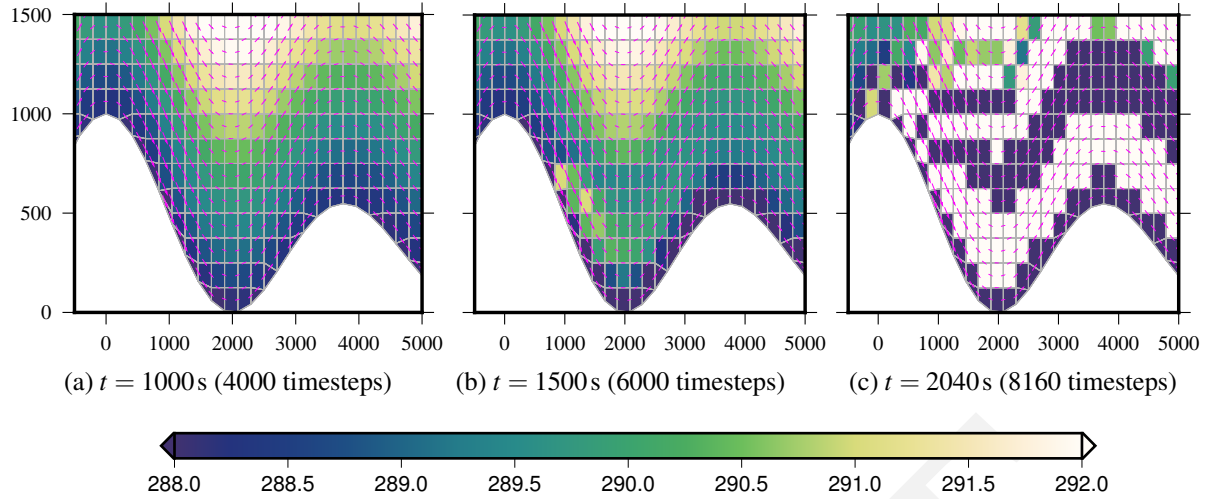


Figure 3: Development of numerical instability in a test of advection of a stratified thermal field in a prescribed, non-divergent wind field that is tangential to basic terrain-following surfaces. Errors are too small to be visible at $t = 1000$ s but, by $t = 1500$ s, erroneously large values have been created near the lower boundary (at $(x, z) = (1000, 600)$ m) that are advected over the lee slopes. By $t = 2040$ s, the instability is fully-developed, having stripes of error and grid-scale oscillations that propagate in a direction opposite to the wind. The timestep is 2.5 s. Cell edges are shown by grey lines. Wind vectors are drawn at every face using magenta arrows, with the wind speed ranging from 10 m s^{-1} to 13 m s^{-1} . Only the lowest 1.5 km of the central domain is shown. The entire domain is 20 km wide and 5 km high. Axis units are m.

4 Future research

My future work begins with the completion of advection scheme development and the submission of a paper on this topic. After that, I intend to resume my research into numerical schemes for generalised Charney–Phillips staggering on arbitrary meshes. MC2 discussed some brief, exploratory work on this topic, but no further work has been done since then. There are a series of tasks that are required to develop numerical schemes for the generalised Charney–Phillips staggering:

1. Define the prognostic variables and their arrangement on arbitrary meshes
2. Design a simple numerical scheme for advecting potential temperature
3. Incorporate the advection scheme into the fully-compressible model from Weller and Shahrokhi (2014), using a fully-explicit configuration
4. Compare the Lorenz and Charney–Phillips variants of the model by selecting test that excite the Lorenz computational model, such as the standing waves tests from Arakawa and Konor (1996)

Following this, further tasks should be undertaken if time permits:

5. Adapt the multidimensional cubic advection scheme for advecting potential temperature on generalised Charney–Phillips meshes
6. Modify the fully-compressible model to enable a semi-implicit configuration with the Charney–Phillips staggering

5 Training

This year, I have attended almost all lunchtime and departmental seminars, HHH and mesoscale group meetings. I take note of analytical techniques that might be useful in future, for example, verifying trends

using low pass filters¹, and solving linear PDEs using Green's functions². I have also peer reviewed a Monthly Weather Review manuscript, and I am keen to get better at critically analysing papers.

Following a talk by Ed Hawkins and Tom Sizmur about online scientific communication, I have been sharing more of my thoughts on my blog and on Twitter³. I have found Twitter to be especially useful for discovering contacts from a range of disciplines whose interests overlap with my research.

Mathematics modules

Spring 2016	MA3NAT	Numerical Analysis II	unassessed
Spring 2015	MAMNSP	Numerical Solution of Partial Differential Equations	78%

RRDP modules

24 Mar 2016	Voice coaching: looking after your voice
26–27 Jan 2016	Preparing to teach (introduction, marking & feedback, leading small groups)
2 Dec 2015	An essential guide to critical academic writing
17 Nov 2015	Understanding the UK higher education context
19 May 2015	How to avoid plagiarism
10 Mar 2015	How to write a literature review
19 Feb 2015	How to write a paper

External courses

June 2016	Dynamical core intercomparison project summer school, NCAR
13 May 2016	Peer review: the nuts and bolts, Sense about Science
June 2015	Advanced numerical methods for Earth-system modelling, ECMWF

Conferences and workshops

October 2016	Speaker	Numerical and computational methods for simulation of all-scale geophysical flows, ECMWF
July 2016	Attendee	1st GungHo Network meeting, Daresbury Laboratory
November 2015	Attendee	GungHo workshop on next generation weather and climate prediction, UK Met Office
June 2015	Attendee	Hoskins@70
June 2015	Poster	SCENARIO DTP conference
March 2015	Speaker	Galerkin methods with applications in weather and climate forecasting, ICMS

Teaching

Oct 2015	Teaching assistant	MTMG02 atmospheric physics
Sep 2015	Teaching assistant	NCAS summer school
Sep 2014	Course teacher	MPE python and linux short course

Visits and collaborations

July 2016	Organising visit from Simon Clark, stratospheric PhD researcher and YouTube vlogger
June 2016 –	Working with Hilary's new MSc student, Christiana Skea, studying variable timestepping for ODEs
June 2016	Visiting NCAR, hosted by Ram Nair
2015 – 2016	Coauthoring an article about dimensionally-split and multidimensional advection schemes, written with Hilary, her former student Yumeng Chen, and Stephen Pring at the UK Met Office

Outreach

14 Jul 2015	Schools physicist of the year awards
14 Jun 2015	East Reading festival
15 Feb 2015	Brighton science festival

¹The summer NAO in observations and CMIP models: impacts on European precipitation and uncertainties in future projected trends, Ileana Bladé, 7 March 2016

²Constraining ocean ventilation pathways and time scales with observations and models, Samar Khatiwala, 21 March 2016

³My blog is at datumedge.co.uk and my Twitter username is @hertzsprrung

Presentations

23 Mar 2016	Quo Vadis	Numerical representation of orography in dynamical cores (honourable mention)
17 Feb 2016	PhD group	Multidimensional advection schemes for arbitrary meshes
9 Feb 2016	Mesoscale group	Curl-free pressure gradients for accurate modelling of cold air pools
19 Oct 2015	HHH group	Improving modelled mountain flows with alternative representations of terrain
27 Apr 2015	HHH group	A like-for-like comparison between terrain following and cut cell grids
21 Apr 2015	PhD group	Discrete vector calculus on Arakawa C grids
12 Feb 2015	UK Met office	Poster presentation
18 Jan 2015	PhD group	Python and linux tips
17 Dec 2014	MPECDT jamboree	Poster presentation
12 Sep 2014	Lunchtime seminar	Gain control of your documents and code: hands-on with revision control and build automation

References

- Almgren, A. S., J. B. Bell, P. Colella, and T. Marthaler, 1997: A Cartesian grid projection method for the incompressible Euler equations in complex geometries. **18**, 1289–1309, doi:10.1137/S1064827594273730.
- Arakawa, A., and C. S. Konor, 1996: Vertical differencing of the primitive equations based on the Charney-Phillips grid in hybrid σ - p vertical coordinates. *Mon. Wea. Rev.*, **124**, 511–528, doi:10.1175/1520-0493(1996)124<0511:VDOTPE>2.0.CO;2.
- Bott, A., 2010: Improving the time-splitting errors of one-dimensional advection schemes in multidimensional applications. *Atmos. Res.*, **97**, 619–631, doi:10.1016/j.atmosres.2010.05.001.
- Clappier, A., 1998: A correction method for use in multidimensional time-splitting advection algorithms: Application to two- and three-dimensional transport. *Mon. Wea. Rev.*, **126**, 232–242, doi:10.1175/1520-0493(1998)126<0232:ACMFUI>2.0.CO;2.
- Ford, R., M. Glover, D. Ham, C. Maynard, S. Pickles, and G. Riley, 2013: GungHo phase 1 computational science recommendations. Tech. Rep. 587, UK Met Office. Available at <http://www.metoffice.gov.uk/media/pdf/8/o/FRTR587Tagged.pdf>.
- Gary, J. M., 1973: Estimate of truncation error in transformed coordinate, primitive equation atmospheric models. *J. Atmos. Sci.*, **30**, 223–233, doi:10.1175/1520-0469(1973)030<0223:EOTEIT>2.0.CO;2.
- Good, B., A. Gadian, S.-J. Lock, and A. Ross, 2014: Performance of the cut-cell method of representing orography in idealized simulations. *Atmos. Sci. Lett.*, **15**, 44–49, doi:10.1002/asl2.465.
- Hartkopf, A. M., 2011: MPFA on polyhedral grids in atmospheric applications. Ph.D. thesis, Martin Luther University of Halle-Wittenberg, available at <http://asam.tropos.de/wp-content/uploads/diplomarbeit.pdf>.
- Jähn, M., O. Knoth, M. König, and U. Vogelsberg, 2015: ASAM v2.7: a compressible atmospheric model with a Cartesian cut cell approach. *Geosci. Model Dev.*, **8**, 317–340, doi:10.5194/gmd-8-317-2015.
- Leonard, B., A. Lock, and M. MacVean, 1996: Conservative explicit unrestricted-time-step multidimensional constancy-preserving advection schemes. *Mon. Wea. Rev.*, **124**, 2588–2606, doi:10.1175/1520-0493(1996)124<2588:CEUTSM>2.0.CO;2.
- Leonard, B., M. K. Macvean, and A. P. Lock, 1993: Positivity-preserving numerical schemes for multidimensional advection. Tech. Rep. 106055, NASA Lewis Research Center. Available at <http://ntrs.nasa.gov/search.jsp?R=19930017902>.
- Lock, S.-J., H.-W. Bitzer, A. Coals, A. Gadian, and S. Mobbs, 2012: Demonstration of a cut-cell representation of 3d orography for studies of atmospheric flows over very steep hills. *Mon. Wea. Rev.*, **140**, 411–424, doi:10.1175/MWR-D-11-00069.1.
- Schär, C., D. Leuenberger, O. Fuhrer, D. Lüthi, and C. Girard, 2002: A new terrain-following vertical coordinate formulation for atmospheric prediction models. *Mon. Wea. Rev.*, **130**, 2459–2480, doi:10.1175/1520-0493(2002)130<2459:ANTFVC>2.0.CO;2.
- Shaw, J., and H. Weller, 2016: Comparison of terrain following and cut cell grids using a non-hydrostatic model. *Mon. Wea. Rev.*, doi:10.1175/MWR-D-15-0226.1, in press.
- Theurich, G., and Coauthors, 2015: The earth system prediction suite: Toward a coordinated U.S. modeling capability. *Bull. Amer. Meteor. Soc.*, doi:10.1175/BAMS-D-14-00164.1, in press.
- Weller, H., and A. Shahrokh, 2014: Curl free pressure gradients over orography in a solution of the fully compressible Euler equations with implicit treatment of acoustic and gravity waves. *Mon. Wea. Rev.*, **142**, 4439–4457, doi:10.1175/MWR-D-14-00054.1.
- Zängl, G., 2012: Extending the numerical stability limit of terrain-following coordinate models over steep slopes. *Mon. Wea. Rev.*, **140**, 3722–3733, doi:10.1175/MWR-D-12-00049.1.